Journal of Cleaner Production 172 (2018) 1212–1223

Contents lists available at ScienceDirect

Journal of Cleaner Production

journal homepage: www.elsevier.com/locate/jclepro

Analytical assessment of asphalt odor patterns in hot mix asphalt production

Federico Autelitano*, Felice Giuliani

University of Parma, Dipartimento di Ingegneria e Architettura, Parco Area delle Scienze, 181/A, 43124, Parma, Italy

ARTICLE INFO

Article history:
Received 21 April 2017
Received in revised form
15 September 2017
Accepted 22 October 2017
Available online 24 October 2017

Keywords:
Asphalt emissions
Pavement engineering
HMA plant
Road construction site monitoring
Artificial olfactory system
Hot recycling in-plant

ABSTRACT

During the various stages of asphalt paving mixtures production and placement, as a result of binder heating, a complex mixtures of hydrocarbons and volatile organic compounds (VOCs) is released into the atmosphere. As far as hot mix asphalt plants is concerned, several standards and directives were drawn up for limiting the emissions of certain specific substances, without setting any specific limit on the odorous perspective. But, odor is increasingly considered an atmospheric pollutant that can have a significant negative impact on both quality of life and economic activity. The odorous flows of HMA emitted in plants or during the paving operations and hot-in-place recycling processes in the worksites can severely limit the usability of the territory. Advances in sensor technology have made possible the development of artificial olfactory systems (AOS), which are devices designed to mimic the human olfactory system capable of characterizing osmogene mixtures. However, their potentialities have not been explored until now at any stages of asphalt and asphalt mixtures production chain. Thus, the main purpose of this study was an analytical-sensory characterization, mainly based on AOS approach, of asphalt emissions generated during the various stages of road pavement construction. The analytical and sensory analyses have firstly demonstrated the effective application of these instruments in the pavement engineering sector: an odor fingerprint of asphalt emissions, specific for each type of binder and temperature class, was determined. Thanks to the photoionization, a technique which allow the detection of organic compounds in gaseous mixtures, a pseudo-hyperbolic relationship between the release of airborne substances in asphalt emissions and the heating temperature was identified; whereas the AOS demonstrated that this increase of VOCs corresponded contextually to a change in their odorous patterns. Moreover, the existence of variations in the odor fingerprints of different asphalt binders heated at the same temperature was assessed. Through a specific statistical approach for the treatment and post-processing of data and the following elaboration of a geometric based procedure for the determination of the numerical inter-class separation, a quantitative value to the purely qualitative response of the AOS was assigned.

1. Introduction

The focus on the atmospheric emissions, particularly the odorous ones, related to industrial production sites and specifically to hot mix asphalt (HMA) manufacturing facilities, was emphasized in the last years, in accordance to the increasing sensitivity towards environment and human health, but also to the growing proximity of emission sources to urban and already settled areas (Belgiorno et al., 2013; Invernizzi et al., 2017). The production of asphalt paving mixtures, consisting of a hot blend of aggregates and asphalt cement, for road pavement construction and maintenance, take place in stationary or mobile plants. Nowadays, there are about 4500 HMA plants both in Europe and in the USA, half of which are also fit for hot and warm recycling (EAPA, 2017; Paranhos and Petter, 2013). Virgin or milled reclaimed asphalt pavement (RAP) aggregates are blended and mixed at about 170–190 °C with hot stored liquid asphalt binder to produce an asphalt paving mixture (Stimilli et al., 2016). The resulting HMA is delivered in properly covered trucks to the paving site, where it is placed and then compacted in a temperature range of 140–160 °C. During storage and handling of asphalt at these elevated temperatures, a complex mixture of predominantly hydrocarbons having a broad boiling

* Corresponding author.
E-mail address: federico.autelitano@unipr.it (F. Autelitano).

https://doi.org/10.1016/j.jclepro.2017.10.248
0959-6526/

point range is released into the atmosphere (Autelitano et al., 2017a; The Asphalt Institute and Eurobitume, 2015). These temperature dependent emissions are a dynamic equilibrium of gases, vapors and mists/aerosols consisting of water, products of combustion (CO_2, NO_x and SO_x), carbon monoxide (CO) and organic compounds of various species, including volatile organic compounds (VOCs) and polycyclic aromatic hydrocarbons (PAHs), some of which may have short- and long-term adverse health effects (EPA, 2000; Ventura et al., 2015). As far as HMA plants is concerned, several standards and directives, all aimed at containing ducted emissions, were drawn up for limiting the emissions of certain specific substances, generally referable to dusts or particulate matters (PM10, PM2.5) and Greenhouse gases (CO_2, NO_x, SO_2), without setting any specific limit on odorous emissions (Almeida-Costa and Benta, 2016; Boczkaj et al., 2014; Jullien et al., 2010; Rubio et al., 2013). Also the scientific literature has generally analyzed asphalt emissions in terms of airborne substances reduction and toxicology risk, related above all to the occupational exposure, ignoring their odorous characteristics (IARC, 2013; Kriech and Osborn, 2014). But, odor is increasingly considered an atmospheric pollutant that can have a significant negative impact on both quality of life and economic activity. The odorous flows of HMA emitted in plants or during the paving operations and hot-in-place recycling processes in the worksites can severely limit the usability of the territory, representing a cause of unquestionable and persistent annoyance for the population living in their vicinity and for workers. Odor emissions are one of the key concerns for the asphalt pavement industry so much so that EAPA (European Asphalt Pavement Association) in Europe and NAPA (National Asphalt Pavement Association) in the USA have set up in recent years technical discussions to address this strategic issue (EAPA, 2014). With only some exception, olfactometry or the measurement of ambient odor concentration has been internationally standardized in recent years only for certain types of facilities (waste, wastewater treatment and composting plants, landfills) (Brancher et al., 2017; Stuchi Cruz et al., 2017; Talaiekhozani et al., 2016).

In the light of the above, there is a need for identifying or developing some instruments and procedures for understanding and systematizing the process of odor generation also for asphalt pavement industry. In general, one of the prerequisites for the evaluation of the odorous emissions feature lies in the identification of the gaseous chemical tracers, which are responsible for their smell. Several consolidated analytical techniques (GC-MS, colorimetric tubes, gas analyzers) have been developed to isolate and characterize the aromatic compounds within the emissions. Such analyses are of fundamental importance to screen and to verify the amount of pollutants emitted into the atmosphere, but they do not provide any information on the odorous sensation produced by the mixture as a whole. In fact, the relationship between physical and chemical properties of the odorant molecules and their olfactory perception, especially for complex gaseous mixtures which are rich in several compounds such as the asphalt ones, is still undergoing research: many airborne compounds could have additive, synergistic or antagonistic/masking effects (Boczkaj et al., 2014; Gasthauer et al., 2008; Porier et al., 2009).

Advances in the field of sensor technology and electronics have made possible the development of devices capable of measuring and recognizing osmogene mixtures characterized by single or complex compounds: the artificial olfactory systems (AOS), also called electronic noses or e-noses (Gardner, 1994; Gardner and Barlett, 1994). The AOS is a biomimetic system that is designed to mimic the human olfactory system in its three fundamental aspects of detection, recording and recognition. The architecture of an electronic nose is significantly depending on the specific application, but it generally consists of three functional components that operate in sequence: a sampling system, an array of gas sensors and a signal-processing system. Thus, this type of instrument collects and processes the responses coming from the sensors; these responses are initially coded as electrical signals and then digitized in order to be numerically processed by a processing system (Boeker, 2014; Pearce et al., 2006). Thanks to specific algorithms, borrowed from the discipline called pattern recognition (PARC), an e-nose constructs an olfactory map (two-dimensional spectral pattern), which does not determine and quantify the individual components present in the odorous mixture but permits the definition of an odorous global feature, the so-called odor fingerprint or smellprint. These algorithms, which are data and signal processing that work sequentially, are generally based on statistical methods (principal component analysis, discriminant factor analysis, analysis of variance between groups, clustering algorithms, etc.) or on artificial intelligence approach (artificial neural networks, Fuzzy logic, genetic algorithm, etc.) (Scott et al., 2006; Villarrubia et al., 2017). Since the first pioneering attempts to measure the volatile compounds in the gaseous mixtures (1950–1960), passing through the development of artificial olfaction technology (1982–1985) and the introduction of the term "electronic nose" (1987–1988), great progress had been made using this approach and such systems had been applied successfully in many areas (Gardner and Barlett, 1994; Pearce et al., 2006; Persaud and Dodd, 1982). Most of the AOS applications relate to food industry (freshness, traceability, adulteration) (Loutfi et al., 2015; Ropodi et al., 2016) and industrial production (QC/QA, manufacturing process, new formulations, packaging) (Deshmukh et al., 2015; Kiani et al., 2016). These devices are very useful in the field of safety (Dobrokhotov et al., 2012), whereas the biomedical (Di Natale et al., 2014; Fitzgerald et al., 2017) and the environmental monitoring (pollution control of water and air) (Capelli et al., 2014; Giungato et al., 2016) represent emerging markets for electronic noses.

Despite discrimination, qualification and monitoring of odors through the AOS approach is a common practice in various industrial sectors, their potentialities have not been explored until now at any stages of asphalt and asphalt mixtures production chain. Only a preliminary warm-up study has demonstrated the possibility of e-nose to discriminate, already at room temperature without the need of sample pre-treatments, between asphalts produced with different origin crude oils and to verify the production stability in the same plant (Autelitano et al., 2017b). Thus, the main purpose of this study was an analytical-sensory characterization, mainly based on AOS approach, of asphalt emissions generated during the various stages of road pavement construction, considering the typical HMA production and paving temperatures. The effect of heating temperature on asphalt emissions was evaluated in terms of variation of both VOCs concentration and odorous patterns (fingerprints), verifying the actual usage, also in this still unexplored field, of a photoionization detector (PID), an instrument which allow the detection of organic compounds in gaseous mixtures, on the one hand and of a portable electronic nose on the other.

2. Materials

The experimental analysis was carried out on four asphalts (penetration grade 70/100), hereinafter referred to as A, B, C and D. Asphalt penetration grade 70/100 is one of the most widely used material in several European countries as a paving grade binder, which is suitable for pavement construction and for the production of other asphalt products. Specifically, asphalts A and C were produced in the same plant refining two different batches of the same

crude oil extracted in the Adriatic basin (Mediterranean Sea); whereas asphalts B and D were obtained in two different refineries by two different Middle-Eastern crude oils. Table 1 summarizes the conventional characteristics of the analyzed asphalts: penetration at 25 °C (EN 1426: 2015) and softening point or ring and ball temperature (EN 1427: 2015).

The relative amounts of asphalt SARA fractions, acronym for saturates, aromatics, resins and asphaltenes, are displayed in Table 2. This analysis was determined by means of thin layer chromatography-flame ionization detection (TLC-FID), according to IP 469/01:2006 standard. The separation was achieved by using a three-stage solvent development sequence: saturates were eluted with heptane, aromatics with a solution of toluene and heptane (80:20 by volume) and resins with a solution of dichloromethane and methanol (95:5 by volume).

3. Methods

The experimental procedure had provided for an odorous identification of the emissions generated by the asphalt heating (range 90–200 °C), in laboratory under controlled conditions (headspace in sealed vials), using a semi-analytical approach and one based on the AOS. The temperature of 90 °C was considered as the lower limit value reported in the literature for road paving applications attributable to warm mix asphalt (WMA) technology, whereas 200 °C represents an extreme upper limit situation potentially observable in plant as a result of asphalt overheating. The headspaces were subjected to a qualitative and semi-quantitative analysis of VOCs by means of photoionization detection (PID) and in parallel to a deepened study of the odorous patterns through the e-nose approach.

3.1. Photoionization detector

VOCs in asphalt emissions were measured by the PhoCheck Tiger 3.1 (Ion science) photoionization detector, which is a hand-held and portable device generally used for gas real-time monitoring and detection (Hori et al., 2015; RAE System, 2013). The instrument uses the high-energy vacuum UV radiation, generated by a 10.6 eV Kr/MgF_2 lamp (comprising a krypton fill gas and a magnesium fluoride window), to photoionize, i.e. to convert into positively charged ions (A^+) and negatively charged electrons (e^-), molecules of chemicals in gaseous or vapor state. Electrons and positive ions are propelled to the electrodes and the resulting small current is amplified by the amplifier chip before being recorded as an output signal (Fig. 1). A chip microcomputer, starting from the PID sensor readings, calculates the VOCs concentrations based on the isobutylene calibration. In general, any chemical compound with ionization energy (IE) lower than that of the lamp photons can be measured. The use of a 10.6 eV lamp had allowed the detection of most of the VOCs present in the asphalt emissions, without interference from major air components (N_2, O_2, CO_2, H_2O) which have higher ionization energies and therefore do not generate any detector's response.

Asphalt specimens (3.000 ± 0.005 g) were put in 50 mL glass vials, which were closed with a butyl stopper and an aluminum crimp cap, and heated at 90, 110, 130, 160 and 180 °C for 20 min. In this analysis, the maximum heating temperature was fixed at 180 °C to avoid the instrument pump failure. The headspace was drawn, using a flow rate of 220 mL/min, into the ionization chamber in which is housed the lamp and the PID sensor. The sampling procedure was based on the use of a flexible extension hose with a disposable 20 G inlet needle ($Ø_{int}$ = 0.90 mm; L = 35 mm) to collect the emissions. PID, using a broad-range detector, provided a single reading for the total detectable VOCs present in the asphalt headspaces. The gas concentration of each specimen, expressed in ppmv, was referred to the sum of 10 consecutive measurements registered in 10 s (1 per sec). The whole dataset was made up of 200 independent measurements: 50 samples (10 for each temperature) for each of the four types of asphalt were prepared, so that each specimen was heated once to the predetermined temperature.

Table 1
Asphalts conventional properties.

Property	Unit	Asphalt			
		A	B	C	D
Penetration (25 °C)	0.1 mm	73	84	75	86
Softening point	°C	49.2	46.4	49.6	46.2

3.2. Analytical-sensor technology: Cyranose® 320

The analytical-sensory analysis of the asphalt emissions generated at high temperatures was conducted by means of the commercially available, portable and hand-held AOS Cyranose® 320 (Cyrano Sciences). The C320 technology lies in its patented NoseChip™, a sensor array of 32 individual thin-film carbon black polymer composite chemiresistors. When the composite film is exposed to a vapor-phase analyte, the polymer matrix swells disrupting the conductive carbon black pathways and consequently increasing the sensors' electrical resistance. Once the analyte is removed, the polymer shrinks to its original size, restoring the conductive pathways. Thus, the measurement cycle provides a three-stage process in which the instrument registers the voltage drop across each sensor and converts it into a resistance reading (R). In the initial phase (baseline purge), necessary for the definition of the baseline resistance (R_0), the ambient air is pulled over the sensors. Then, in the sampling phase (sample draw) the chemical vapors reach the NoseChip™ for the sample detection. Finally, after the sample removal, the gas stream is emitted at the instrument exhaust port and clean air is carried to the sample chamber to refresh the sensors (purge air intake) and to purge the pneumatic system of any residual sample vapors (purge sample intake), restoring the initial configuration (Fig. 2). The relative change in the resistance for each of the 32 sensors (sample draw vs baseline purge) was captured as raw datum, also defined sensor response signature, which was then converted to the maximum relative change in resistance caused by the analyte exposure to the sensors ($(R_{max}-R_0)/R_0$). The graphical representation of the sensor response signatures describe the so called smellprint, which is unique for each analyte.

The preliminary and necessary phase of initial calibration has led to the definition of a specific test protocol, described in Table 3. Asphalt samples (3.000 ± 0.005 g) were placed in 50 mL glass vials hermetically sealed with a butyl stopper and an aluminum crimp cap. The vials were then heated for 20 min in a static oven at different temperatures (90, 110, 130, 160 and 200 °C). Once removed from the oven, they were maintained for 120 min at 22 ± 1 °C, temperature at which occurred the sampling of the headspace by means of a disposable 20 G needle ($Ø_{int}$ = 0.90 mm; L = 35 mm). This choice was due to the fact that sampling vapors at temperatures higher than ambient temperature, vapors may condensate in the pneumatic pathway or on the sensors affecting the performance of the C320. A vent 23 G needle ($Ø_{int}$ = 0.60 mm; L = 30 mm) was inserted into the septum to equilibrate the internal pressure during the sample draw. The vent needle and the sample needle were kept sufficiently far apart so that the sample was not diluted with ambient air during the analysis. A charcoal filter was used to

Table 2
Asphalts SARA fractions: mean and standard deviation (n = 20).

Fraction	Unit	Asphalt			
		A	B	C	D
Saturates (470–880 g/mol)	%	5.7 (0.4)	5.2 (0.4)	5.8 (0.2)	2.3 (0.2)
Aromatics (570–980 g/mol)	%	48.6 (1.7)	52.6 (2.7)	45.5 (1.6)	55.3 (2.0)
Resins (800–2000 g/mol)	%	20.9 (0.9)	26.6 (1.7)	25.9 (0.6)	25.5 (1.8)
Asphaltenes (800–3500 g/mol)	%	24.8 (0.8)	15.6 (1.2)	22.8 (1.1)	16.9 (0.7)

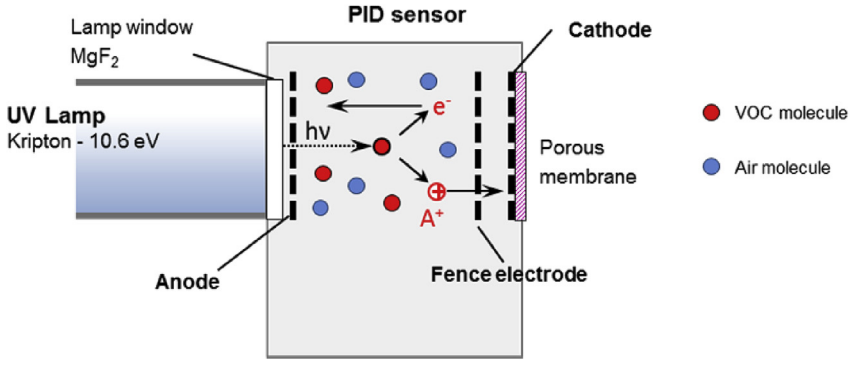

Fig. 1. PID principle of operation.

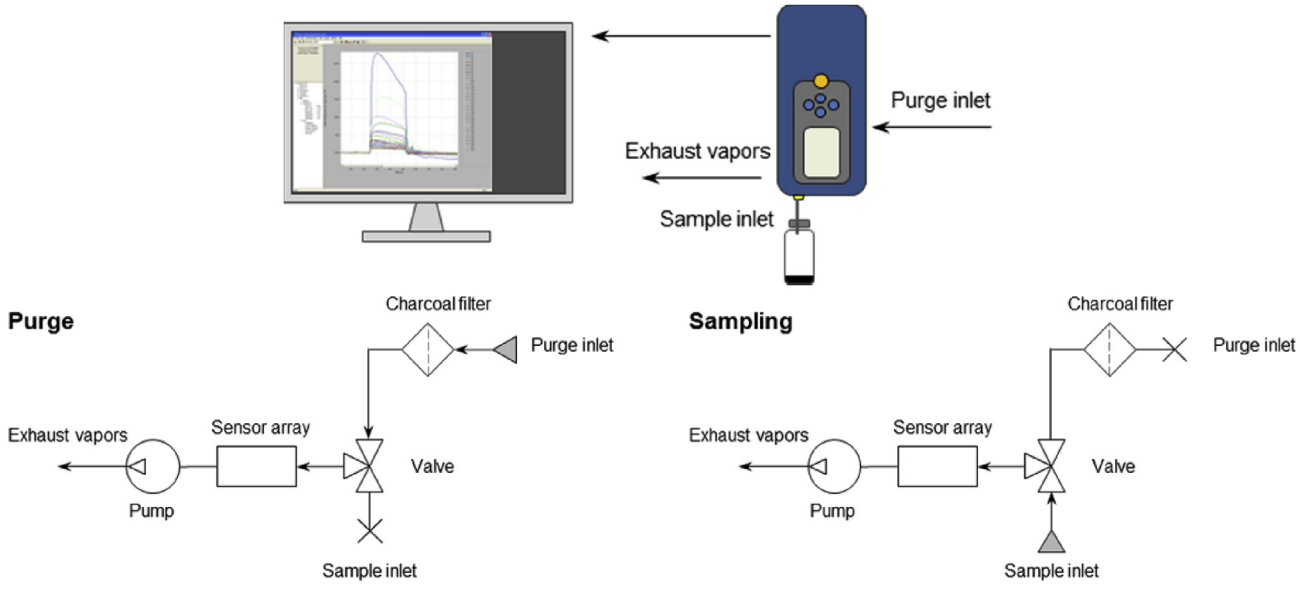

Fig. 2. Cyranose® 320 principle of operation.

Table 3
Acquisition method of Cyranose® 320.

Flow settings	Time [sec]	Flow [mL/min]
Baseline purge	30	120
Sample draw	25	120
1st sample gas purge	120	180
1st air intake purge	50	180
2nd sample gas purge	20	180
2nd air intake purge	20	180

eliminate the variability of possible organic contaminants in the ambient air. The temperature of the sensor array substrate was set and maintained at 41 °C.

The whole data set, as well as for the photoionization analysis, was constituted by 200 independent measurements: 10 specimens for each of the five temperatures for each of the four types of asphalt. The data were then statistically processed through the principal component analysis (PCA), performed with a specifically developed MATLAB R2016b script, to depict differences in the odorous patterns of the asphalt emissions. Specifically, PCA is an unsupervised multivariate procedure based on the dimension reduction of the dataset, consisting of a large number of interrelated variables, by transforming to a new set of uncorrelated variables, precisely the principal components (PCs), while maintaining as much as possible the variation present in the dataset (Jolliffe, 2002).

One common criteria for determining how many PCs should be investigated and how many should be ignored is to include all those PCs up to a predetermined total percent variance explained, such as generally 90%. Once identified the lowest-dimensional PCs hyperplane that best satisfied this condition, the inter-class separation was analytically determined, calculating the numerical distance in terms of Euclidean distance between two classes. Fig. 3 schematically summarizes all the geometric parameters used for this analysis, referring to two hypothetical classes Ω and Φ in a two-dimensional space. The Euclidean distance ($\overline{G_{\Omega,\Phi}}$) and the distance along the two axes ($\overline{G1_{\Omega,\Phi}}$ and $\overline{G2_{\Omega,\Phi}}$) were determined considering as reference the center of gravity (G1, G2) of each class. As for the uncertainties of the measurements, there is to consider that the sensors adopted are sensitive to small variations of the environmental conditions and the response of the system could have drift of different nature even though a careful instrument conditioning before each run was required. Considering only the electronics, the uncertainties due to, e.g. resistivity variation of the sensors, accidental error caused by imperfect cleaning, eventually cross-talking amongst sensors and other possible interferences or spurious effects were considered. However, all these uncertainties are minor with respect to the repeatability of measurements (measurements executed with the same sample within a short time interval) which is intrinsic to the actual technology level. As a measure of uncertainty (intra-class distance) standard deviations were assumed: standard deviation along PC1-axis (σ(G1)), PC2-axis (σ(G2)) and the square root of the sum of the square standard deviation along PC1-axis and PC2-axis ($\sigma(G1G2) = \sqrt{(\sigma(G1))^2 + (\sigma(G2))^2}$). They contain all the indications on the various effects able to influence measurements executed with the same procedure on the same material, treated in the same way.

4. Results

The photoionization analyses have allowed to quantify the VOCs

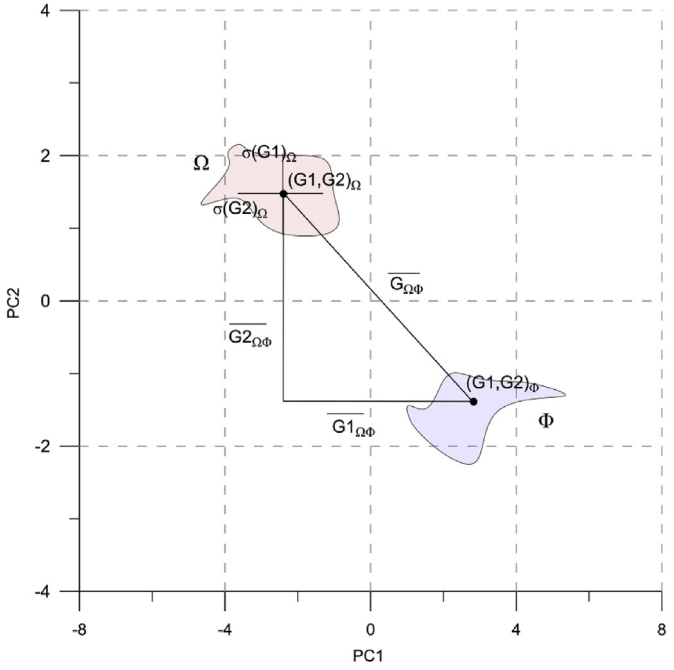

Fig. 3. Geometric parameters used in PCA.

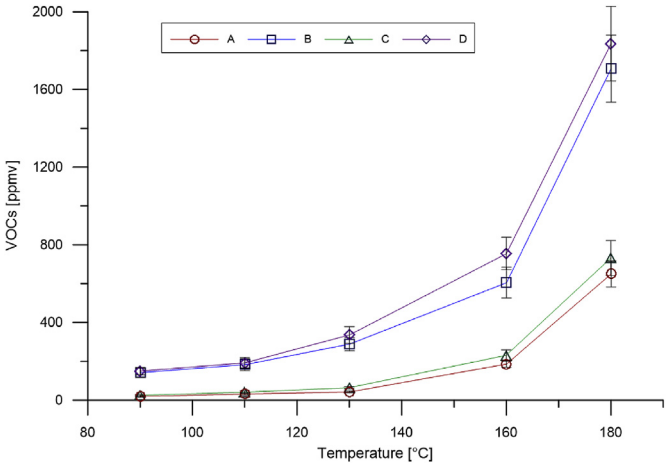

Fig. 4. PID responses (VOCs concentration) vs temperature in asphalt headspaces.

concentration in the asphalt headspaces generated at different temperatures (Fig. 4). An increase of PID response was highlighted with increasing temperature, more significant for temperatures higher than 130 °C, that is, those typical of production and placement of traditional HMA mixtures. A variation of approximately 3000% was observed passing from 90 to 180 °C (incremental ratio of about 30) for asphalt A and C, while of 1000% for B and D (incremental ratio of about 10). These values, however, appear to be strongly influenced by those detected at 90 °C, considerably lower for asphalts A and C, characterized by a greater content of the asphaltene fraction (highly polar aromatic compounds having high molecular mass). Asphalts A and C have in fact shown a lower VOCs concentration in the headspace compared to asphalt B and D, richer in more volatile compounds (saturated and aromatic), quantifiable in 80% up to 130 °C and in 60% for the higher temperatures.

A variety of curve-fitting methods, in both linear and nonlinear regression, was evaluated to model the PID acquired data. Among over 90 models, a pseudo-hyperbolic relationship between the emissions generated by the asphalt binder (in terms of VOCs) and the heating temperature (in the typical temperature range registered in the various stages of road pavement construction) was identified as the best fit model, according to the function (Mian, 1992):

$$y = q_0\left(1+\frac{bx}{a}\right)^{\left(-\frac{1}{b}\right)} \rightarrow VOC = q_0\left(1+\frac{bT}{a}\right)^{\left(-\frac{1}{b}\right)} \quad (1)$$

where q_0, a and b are the parameters of the interpolated curve, while T represents the temperature. The numerical values of the parameters (Table 4) clearly show how the increase in emissions was significantly higher for asphalts B and D.

Once measured the amount of VOCs in the asphalt emissions, the main objective was to assess whether the increase in the airborne substances corresponded contextually to a change in their

Table 4
Parameters of the interpolated curves.

Parameter	Asphalt			
	A	B	C	D
q_0	2.929	64.020	4.269	48.948
a	−68.030	−145.697	−69.641	−105.840
b	0.305	0.738	0.367	0.488
R^2	0.999	0.999	0.999	0.999

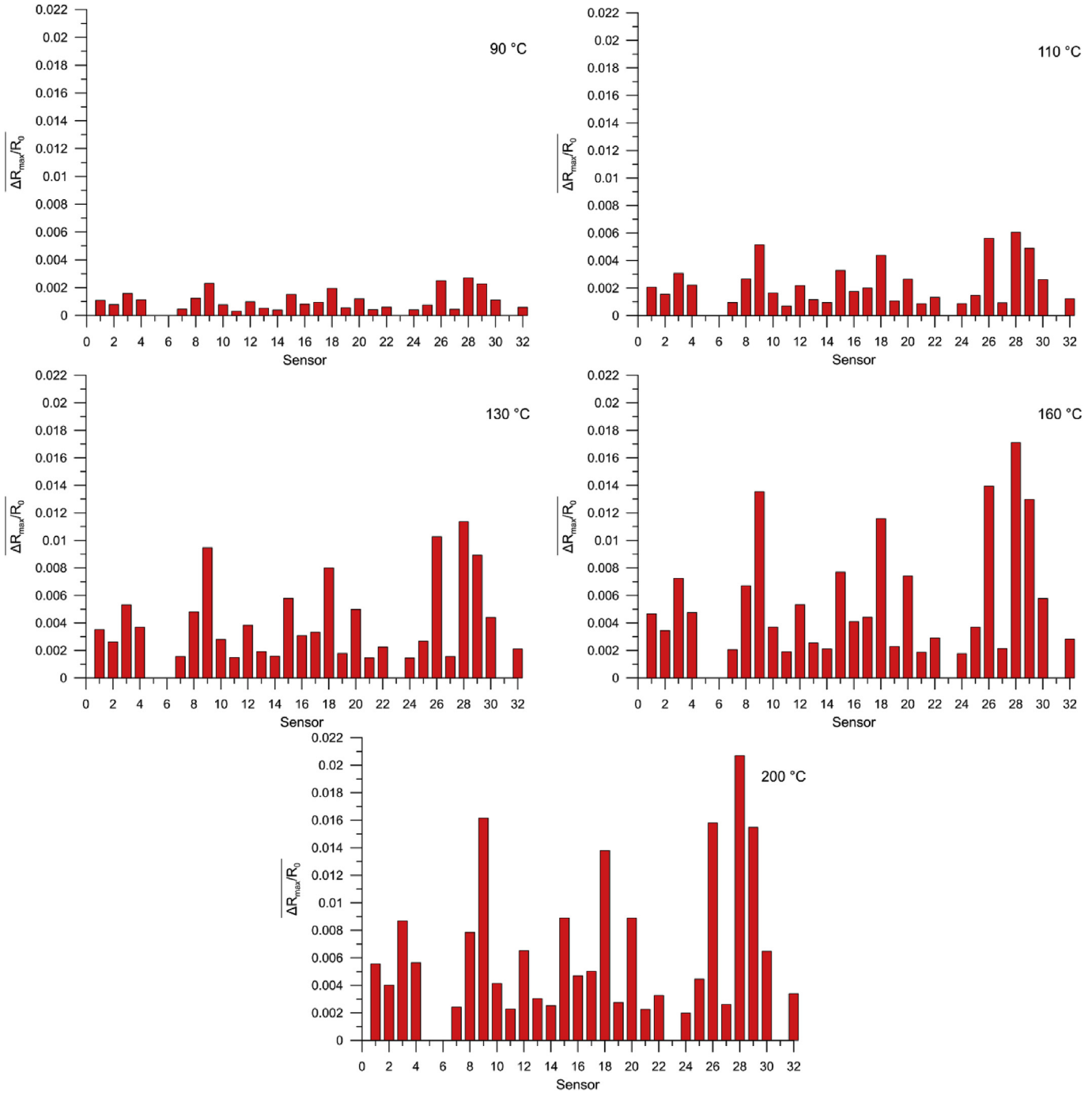

Fig. 5. Bar graph of the response signature for asphalt A at 90, 110, 130, 160 and 200 °C.

odorous patterns. The raw data measured with Cyranose® 320, stored as change in sensor resistance ($\Delta R/R_0 \cdot 10^6$) as a function of time, were converted into the maximum relative resistance change caused by the analyte exposure recorded during sample draw and baseline purge stages ($\Delta R_{max}/R_0$). These sensor signatures were represented using a histogram which allows to define the odor fingerprint of asphalt at different temperatures in the form of a bar graph. The vertical axis represents the sensor maximum relative resistance change, calculated as mean value of 10 samples for each temperature class ($\overline{\Delta R_{max}/R_0} = \frac{1}{10}\sum_{i=1}^{10}\frac{R_{max,i}-R_{0,i}}{R_{0,i}}$), whereas the sensor numbers are plotted along the horizontal axis. Discrimination was improved by deselecting four sensors (5, 6, 23 and 31) that are sensitive to water and changes in humidity, as a standard practice in the literature (Bikov et al., 2004; Mohapatra et al., 2015). The thermal conditioning procedure, as described, has provided for the heating of the asphalt samples in hermetically closed vials. During the cooling phase, even if conducted very carefully and gradually in the temperature transition, small quantities of condensate may have formed, capable of altering the correct excitation process of these four sensors in contact with the vapor phase and accordingly the statistical treatment of data in the post-processing phase.

Fig. 5, by way of example, represents the fingerprints of asphalt

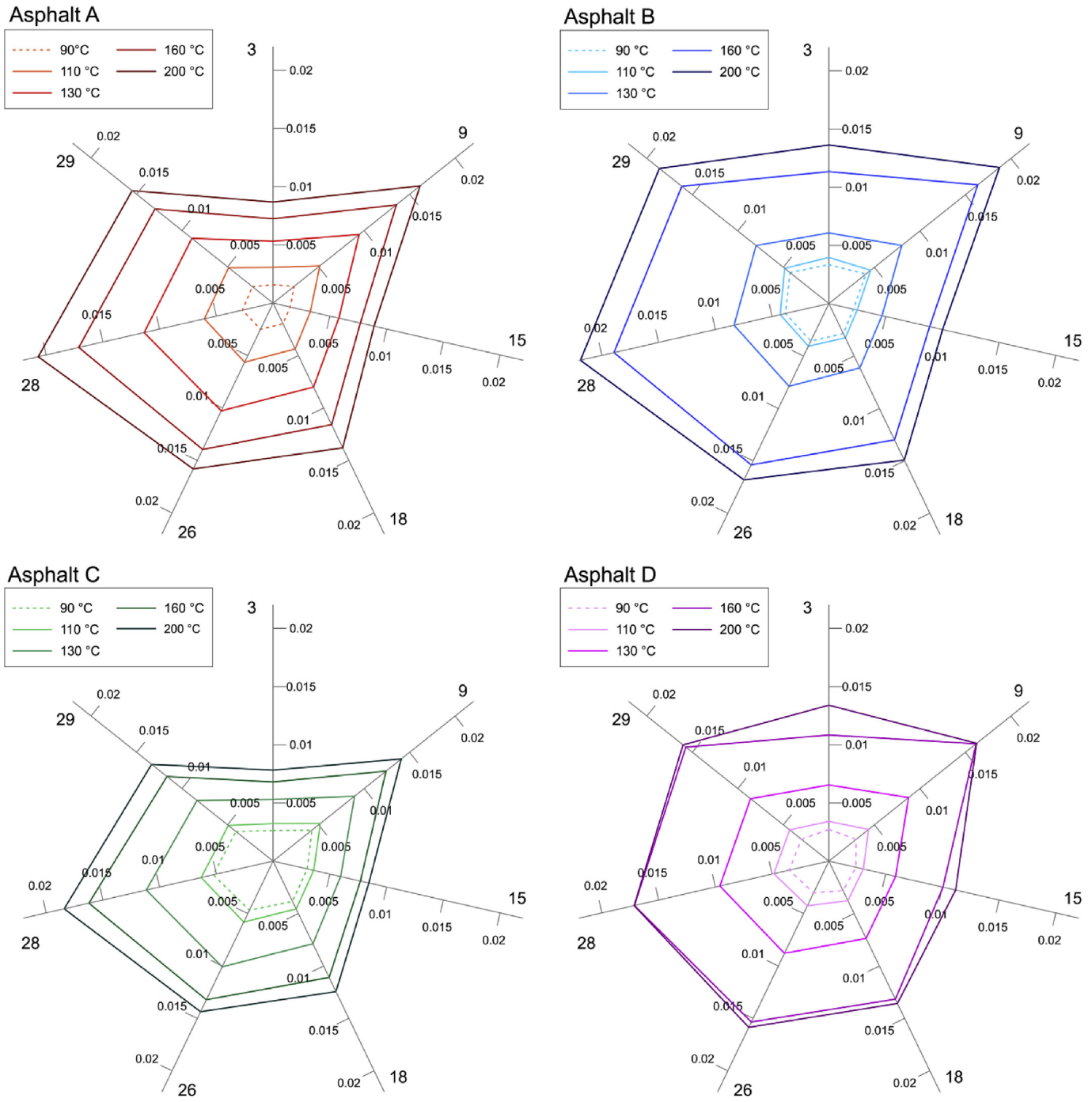

Fig. 6. Radar plot of the response signature of seven sensors at different temperatures.

A at different heating temperatures. The bar graphs show a growing trend in the sensors response with the increase of temperature. Such behavior, which was recorded for all asphalts, can be made more visible using radar plots. These graphs display in a two-dimensional space the sensors response in terms of $\overline{\Delta R_{max}/R_0}$ on each axis. To make this graphical representation more understandable and readable, seven sensors (number 3, 9, 15, 18, 26, 28 and 29) that have interacted more significantly with the asphalt emissions were considered (Fig. 6). As can be seen, the polygon representative of a temperature is always circumscribed by that relative to the higher temperature, according to a sequential order. This trend demonstrates an increase in the chemical interaction between asphalt vapor-phase and sensors film with increasing temperature.

The response of the 28 sensors was then normalized, using the variance as standardization parameter, to remove the effects of response size. The normalized values were then subjected to PCA: for each asphalt, analyzed independently of the others, five temperature classes were considered. The percentage of the total explained variance by the first two principal components (PC1 and PC2) was greater than 99%. Specifically, only PC1 would have been able to explain more than 99% of the variance in all the considered

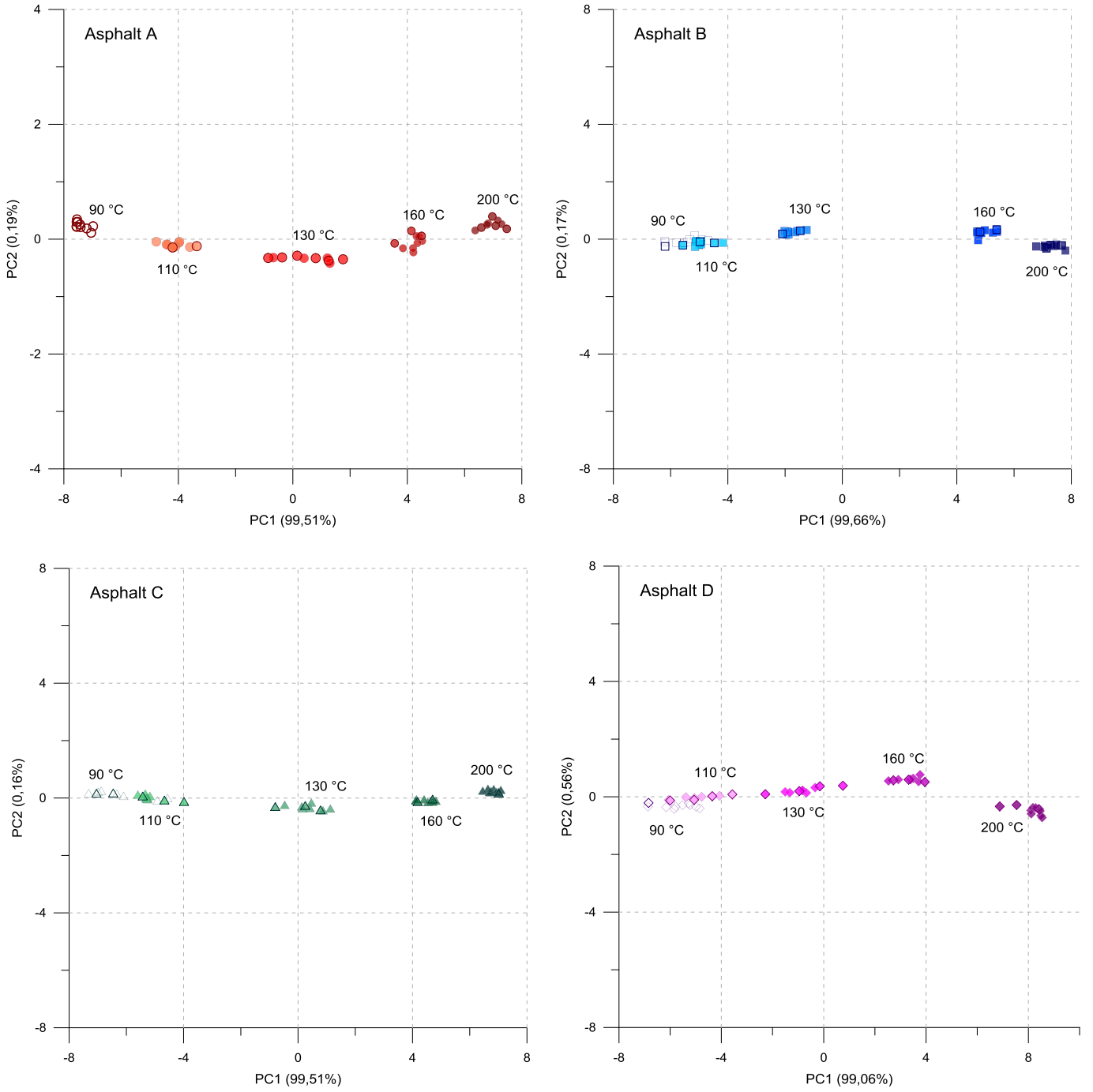

Fig. 7. Two-dimensional PCA plot for the asphalts as a function of temperature.

cases. Furthermore, the Euclidean distances calculated to the origin of the reference system, considering both a bi- and a tri-dimensional space never deferred for more than 1%. Thus, the statistical analysis considered the first two principal components. The representation on the two-dimensional space PC1-PC2 describes the influence of the temperature parameter on the asphalt emissions odorous patterns (Fig. 7).

The trend was rather homogeneous for all asphalts: the cloud of data representative the five classes of temperature (90, 110, 130, 160 and 200 °C) were clustered and arranged in ascending order along the PC1 axis. The increase in the heating temperature translates into a sub-horizontal shift to the right. In fact, a significant change in the center of gravity position of each data cloud was highlighted only for the PC1 coordinate, towards the positive PC1-axis. With the exception of a partial overlap of the classes 90 °C and 110 °C (except for asphalt A), a clear separation between the other temperatures was registered. The numerical values of the inter-class separation referred to each asphalt (Table 5) demonstrate how the discrimination for each pair of temperature classes was confirmed by the fact that the Euclidean distances ($\overline{G_{T,T+1}}$) between the centers of gravity were much greater than the sum of the standard deviations of the relative areas ($\sigma(G1G2)_T+\sigma(G1G2)_{T+1}$). The square root of the sum of the variances of two data clouds

Table 5
PCA geometric parameters relative to asphalts at different temperatures.

Asphalt	T [°C]	G1	G2	σ(G1)	σ(G2)	σ(G1G2)	$\overline{G1_{T,T+1}}$	$\overline{G2_{T,T+1}}$	$\overline{G_{T,T+1}} \pm \sigma(G1G2)^{*}_{T,T+1}$
A	90	−7.38	0.24	0.22	0.07	0.23	–	–	–
	110	−4.10	−0.10	0.41	0.04	0.41	3.28	0.34	3.30 ± 0.47
	130	0.49	−0.34	0.91	0.05	0.91	4.59	0.24	4.60 ± 1.00
	160	4.21	−0.04	0.30	0.12	0.32	3.71	0.30	3.73 ± 0.97
	200	6.78	0.25	0.64	0.07	0.64	2.57	0.29	2.59 ± 0.72
B	90	−5.54	−0.07	0.54	0.10	0.55	–	–	–
	110	−4.94	−0.14	0.38	0.07	0.39	0.60	0.07	0.60 ± 0.67
	130	−1.77	0.24	0.27	0.06	0.28	3.17	0.39	3.20 ± 0.48
	160	4.96	0.22	0.28	0.10	0.30	6.73	0.02	6.73 ± 0.41
	200	7.29	−0.25	0.30	0.06	0.31	2.33	0.48	2.38 ± 0.43
C	90	−6.47	0.14	1.07	0.11	1.08	–	–	–
	110	−5.13	0.02	0.47	0.09	0.48	1.34	0.12	1.34 ± 1.18
	130	0.30	−0.31	0.59	0.08	0.59	5.43	0.33	5.44 ± 0.76
	160	4.49	−0.09	0.26	0.04	0.27	4.20	0.22	4.20 ± 0.65
	200	6.81	0.24	0.20	0.05	0.20	2.32	0.33	2.34 ± 0.33
D	90	−5.73	−0.32	0.71	0.07	0.72	–	–	–
	110	−4.87	−0.02	0.81	0.07	0.81	0.87	0.30	0.92 ± 1.08
	130	−0.81	0.22	0.82	0.10	0.83	4.05	0.25	4.06 ± 1.16
	160	3.32	0.60	0.46	0.07	0.47	4.13	0.37	4.15 ± 0.95
	200	8.10	−0.43	0.52	0.14	0.54	4.78	1.07	4.90 ± 0.71

$^{*}\sigma(G1G2)_{T,T+1} = \sqrt{\sigma(G1G2)^2_T + \sigma(G1G2)^2_{T+1}}$.

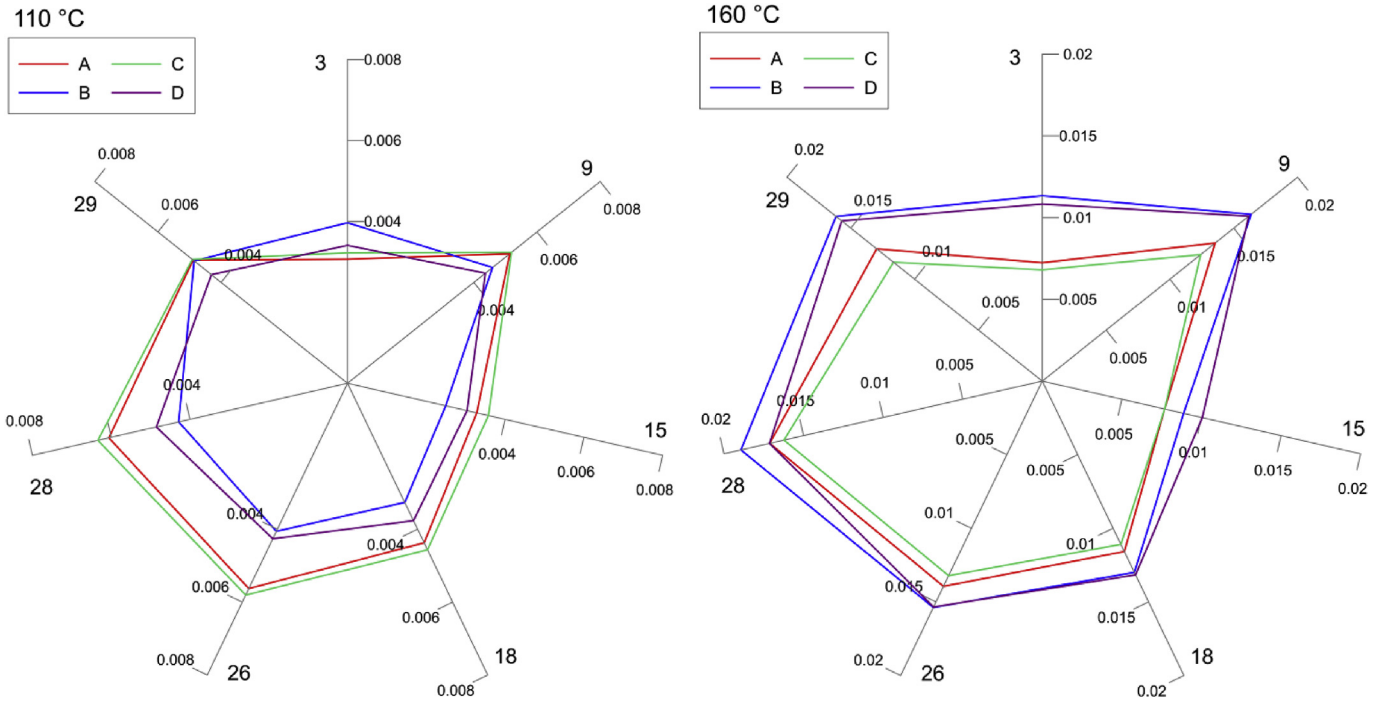

Fig. 8. Radar plot of the response signature of seven sensors at 110 °C and 160 °C.

$(\sigma(G1G2)_{T,T+1} = \sqrt{(\sigma(G1G2)_T)^2 + \sigma(G1G2)^2_{T+1}})$ was assumed as an estimator of the uncertainty. The confidence level is obtained by multiplying this standard deviation of the distance with a coefficient computed according to a Student's t distribution.

Once identified a significant difference in the smell of the emissions as a function of temperature, the existence of variations in the odorous profile of different asphalt binders heated at the same temperature was verified. As an example Fig. 8, relative to 110 °C and 160° C, shows how each asphalt caused different sensors responses.

In fact, with the exception of the asphalt pair A and C (refined in the same plant from two different batches of the same crude oil), the response of the seven most excited sensors tracks polygons with different shape and size. Thus, such behavior underlies a different excitation process, symptom of specific and peculiar odorous patterns characterizing the emissions generated by different asphalt binders.

The normalized responses of the 28 sensors were statistically treated using PCA. Five independent analyses were conducted, each relating to a specific heating temperature, in which the classes were represented by the four asphalts. Also in this case, the low-dimensional hyperplane that best summarizes all the variation in the 28 sensors response matrix was represented by the first two principal components. Fig. 9 shows the 2D-PCA plots concerning the four asphalts for all the considered temperatures (90, 110, 130,

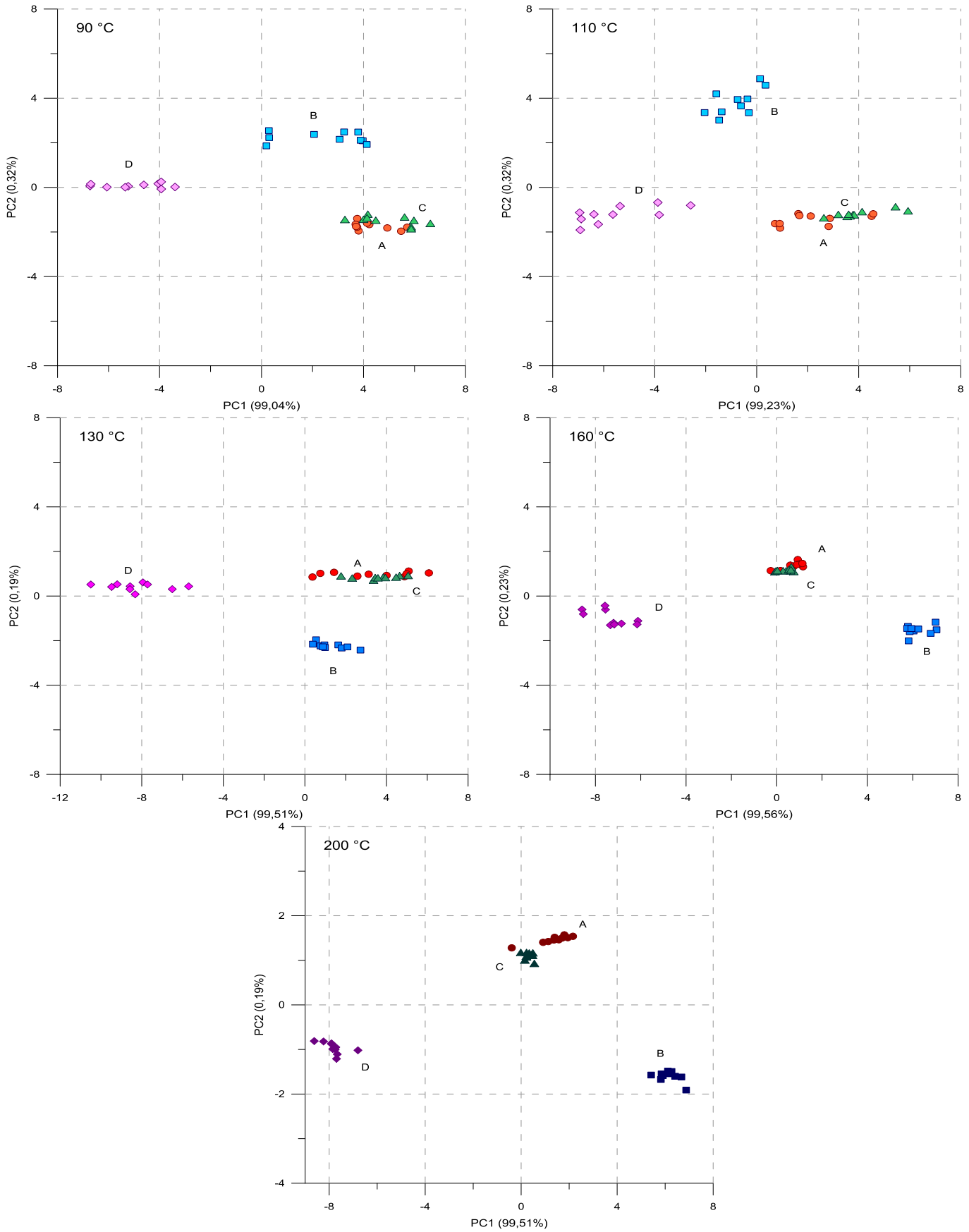

Fig. 9. 2D-PCA plot concerning the four asphalts for all the considered temperatures.

Table 6
Asphalt interclass distances at 160 °C.

Asphalt	G1	G2	Distance	Asphalt			
				A	B	C	D
A	0.70	1.36	$\overline{G1_{A,\Phi}}$	0.45[a]	5.53	0.32	8.01
			$\overline{G2_{A,\Phi}}$	0.15[a]	2.88	0.20	2.34
			$\overline{G_{A,\Phi}}$	0.47[a]	6.24 ± 0.73[b]	0.38 ± 0.57[b]	8.35 ± 1.04[b]
B	6.23	−1.53	$\overline{G1_{B,\Phi}}$		0.52[a]	5.85	13.54
			$\overline{G2_{B,\Phi}}$		0.22[a]	2.68	0.54
			$\overline{G_{B,\Phi}}$		0.56[a]	6.44 ± 0.65[b]	13.55 ± 1.08[b]
C	0.38	1.15	$\overline{G1_{C,\Phi}}$			0.31[a]	7.69
			$\overline{G2_{C,\Phi}}$			0.06[a]	2.14
			$\overline{G_{C,\Phi}}$			0.31[a]	7.98 ± 0.97[b]
D	−7.31	−0.98	$\overline{G1_{D,\Phi}}$				0.84[a]
			$\overline{G2_{D,\Phi}}$				0.38[a]
			$\overline{G_{D,\Phi}}$				0.92[a]

[a] Value referred to the standard deviation.
[b] $\sigma(G1G2)_{\Omega,\Phi} = \sqrt{\sigma G1G2_{\Omega}^2 + \sigma G1G2_{\Phi}^2}$

160 and 200 °C).

The numerical inter-class discrimination followed the same procedure illustrated above: the Euclidean distance, including uncertainty ($\overline{G_{\Omega,\Phi}} + \sqrt{(\sigma(G1G2)_{\Omega}^2 + \sigma(G1G2)_{\Phi}^2}$) and the distance along both axes ($\overline{G1_{\Omega,\Phi}}$ and $\overline{G2_{\Omega,\Phi}}$) were determined considering as reference the center of gravity of each asphalt class. In Table 6, the temperature of 160 °C is given as an example.

The graphs and the numerical values show a significant separation between the clouds of data representing the various asphalts, with the exception of the pair A-C for which there is a nearly complete overlap. This behavior was found for all the considered temperatures: the inter-class distances were much greater than the sum of the standard deviations of the relative areas. In this case there is not only a horizontal spatial separation between the classes, i.e. along the PC1 component, but also vertically, along the PC2 component. In general, data for higher temperatures (160 °C and 200 °C), were more tightly clustered than the data for lower temperature, highlighting how a greater excitation of the sensors has permitted a better PARC process.

5. Conclusions

During the various stages of asphalt paving mixtures production and placement, as a result of the asphalt heating, gaseous blends characterized by an intrinsic complexity of substances and compounds are emitted into the atmosphere. The photoionization analyses confirmed as temperature represents the crucial factor in the generation of such emissions. A pseudo-hyperbolic relationship between the release of airborne substances, in the form of VOCs, and the heating temperature was identified. Specifically, a significant increase in asphalt emissions was registered for temperatures greater than 130 °C, that is, those typical of production and placement of traditional HMA mixtures. Moreover, a positive correlation between the amount of VOCs in the headspaces and the content of the more volatile fractions (saturated and aromatic) in the asphalt solid matrix was revealed. Thus, the possibility to compare continually the PID readings with previously set alarm exposure levels, which are specific for each hazardous environment, makes this type of instruments a useful and interesting cost-effective solution also in the asphalt pavement industry for monitoring the potential release of pollutant compounds in some crucial phases of HMA production processes.

The sensory analyses conducted using the Cyranose® 320 have firstly allowed to demonstrate the effective application of AOS in the pavement engineering sector and in the monitoring of HMA plants and road construction sites, thanks to the far from obvious compatibility between the sensors' operating principle and the odor of asphalt emissions. A specific and peculiar odor fingerprint was determined for each type of asphalt binder and temperature class. Through a specific statistical approach for the treatment and post-processing of data (PCA) and the following elaboration of a geometric based procedure for the determination of the numerical inter-class separation, a quantitative value to the purely qualitative response of the electronic nose was assigned. A growing trend in the sensors response with heating temperature was identified, demonstrating an increase in the chemical interaction between asphalt vapor-phase and sensors film with temperature rise. With the exception of a partial overlap of the classes 90 °C and 110 °C (temperatures referable to WMA mixtures placement), a clear separation between the other temperatures was registered. This trend, coupled to the PID results, testifies a change in the odorous patterns contextually to the increase of volatile substances emission. Once identified a significant difference in the smell of the emissions as a function of temperature, the existence of variations in the odorous profile of different asphalt binders heated at the same temperature was assessed. Specifically, the AOS was able to discriminate the odor of asphalt emissions generated by heating commercially identical binders produced from different crude oils. Furthermore, a remarkable aspect linked to the control and the guarantee of in-plant production stability, involved the individuation of almost overlapping odor patterns between asphalts refined in the same plant from different batches of the same crude oil.

Thus, all these findings represent a valid starting point for the development of standardized procedures and methodologies based on the principle of the electronic nose to recognize the smell generated during the different stages of production and laying of asphalt mixtures to which associate nuisance limits or olfactory annoyance. This possibility arises from the commercial availability of different type of sensors with high and different sensitivities to a wide range of organic vapors, which would allow the construction of a trained multisensor array calibrated on the specific needs of asphalt pavement industry.

Appendix A. Supplementary data

Supplementary data related to this article can be found at https://doi.org/10.1016/j.jclepro.2017.10.248.

References

Almeida-Costa, A., Benta, A., 2016. Economic and environmental impact study of warm mix asphalt compared to hot mix asphalt. J. Clean. Prod. 112, 2308–2317.

Autelitano, F., Bianchi, F., Giuliani, F., 2017a. Airborne emissions of asphalt/wax blends for warm mix asphalt production. J. Clean. Prod. 164, 749–756.

Autelitano, F., Garilli, E., Pinalli, R., Montepara, A., Giuliani, F., 2017b. The odour fingerprint of bitumen. Road Mater. Pavement Des. 18 (Suppl. 2:EATA 2017), 178–188.

Belgiorno, V., Naddeo, V., Zarra, T., 2013. Odour Impact Assessment Handbook. John Wiley & Sons, Chichester.

Bikov, A., Hernadi, M., Korosi, B.Z., Kunos, L., Zsamboki, G., Sutto, Z., Tarnoki, A.D., Tarnoki, D.L., Losonczy, G., Horvath, I., 2004. Expiratory flow rate, breath hold and anatomic dead space influence electronic nose ability to detect lung cancer. BMC Pulm. Med. 14 (202).

Boczkaj, G., Przyjazny, A., Kamiński, M., 2014. Characteristics of volatile organic compounds emission profiles from hot road bitumens. Chemosphere 107, 23–30.

Boeker, P., 2014. On 'electronic nose' methodology. Sensors Actuators B 204, 2–17.

Brancher, M., Griffiths, K.D., Franco, D., de Melo Lisboa, H., 2017. A review of odour impact criteria in selected countries around the world. Chemosphere 168, 1531–1570.

Capelli, L., Sironi, S., Del Rosso, R., 2014. Electronic noses for environmental monitoring applications. Sensors 14 (11), 19979–20007.

Deshmukh, S., Bandyopadhyay, R., Bhattacharyya, N., Pandey, R.A., Jana, A., 2015. Application of electronic nose for industrial odors and gaseous emissions measurement and monitoring - an overview. Talanta 144, 329–340.

Di Natale, C., Paolesse, R., Martinelli, E., Capuano, R., 2014. Solid-state gas sensors for breath analysis: a review. Anal. Chim. Acta 824, 1–17.

Dobrokhotov, V., Oakes, L., Sowell, D., Larin, A., Halla, J., Kengne, A., Bakharev, P., Corti, G., Cantrell, T., Prakash, T., Williams, J., McIlroy, D.N., 2012. Toward the nanospring-based artificial olfactory system for trace-detection of flammable and explosive vapors. Sensors Actuators B 168, 138–148.

EAPA, 2014. EAPA Newsletter. Issue 32. European Asphalt Pavement Association, Brussels.

EAPA, 2017. Asphalt in Figures 2015. European Asphalt Pavement Association, Brussels.

EPA, 2000. Hot Mix Asphalt Plant. Emission assessment report (EPA 454/R-00-019). U.S. Environmental Protection Agency, Research Triangle Park.

Fitzgerald, J.E., Bui, E.T.H., Simon, N.M., Fenniri, H., 2017. Artificial nose technology: status and prospects in diagnostics. Trends Biotechnol. 35 (1), 33–42.

Gardner, J.W., 1994. Detection of vapours and odours from a multisensor array using pattern recognition: principal component and cluster analysis. Sensors Actuators B Chem. 4, 109–115.

Gardner, J.W., Barlett, P.N., 1994. Brief history of electronic nose. Sens. Actuator B 18, 211–220.

Gasthauer, E., Mazé, M., Marchand, J.P., Amouroux, J., 2008. Characterization of asphalt fume composition by GC/MS and effect of temperature. Fuel 87, 1428–1434.

Giungato, P., de Gennaro, G., Barbieri, P., Briguglio, S., Amodio, M., de Gennaro, L., Lasigna, F., 2016. Improving recognition of odors in a waste management plant by using electronic noses with different technologies, gas chromatography-mass spectrometry/olfactometry and dynamic olfactometry. J. Clean. Prod. 133, 1395–1402.

Hori, H., Ishimatsu, S., Fueta, Y., Hinoue, M., Ishidao, T., 2015. Comparison of sensor characteristics of three real-time monitors for organic vapors. J. Occup. Health 57 (1), 13–19.

IARC, 2013. Bitumens and Bitumen Emissions, and Some N- and S-heterocyclic Polycyclic Aromatic Hydrocarbons, vol. 103. International Agency for Research on Cancer Monograph, Lyon.

Invernizzi, M., Capelli, L., Sironi, S., 2017. Proposal of odor nuisance index as urban planning tool. Chem. Senses 42 (2), 105–110.

Jolliffe, I.T., 2002. Principal Component Analysis, second ed. Springer, New York.

Jullien, A., Gaudefroy, V., Ventura, A., de la Roche, C., Paranhos, R., Monéron, P., 2010. Airborne emissions assessment of hot asphalt mixing: methods and limitations. Road Mater. Pavement Des. 11 (1), 149–169.

Kiani, S., Minaei, S., Ghasemi-Varnamkhasti, M., 2016. Application of electronic nose systems for assessing quality of medicinal and aromatic plant products: a review. J. Appl. Res. Med. Aromatic Plants 3 (1), 1–9.

Kriech, A.J., Osborn, L.V., 2014. Review and implications of IARC monograph 103 outcomes for the asphalt pavement industry. Road Mater. Pavement Des. 15 (2), 406–419.

Loutfi, A., Coradeschi, S., Mani, G.K., Shankar, P., Rayappan, J.B.B., 2015. Electronic noses for food quality: a review. J. Food Eng. 144, 103–111.

Mian, M.A., 1992. Petroleum Engineering Handbook for Practicing Engineer, vol. 1. Penn Well Publishing Company, Tulsa.

Mohapatra, P., Panigrahi, S., Amamcharla, J., 2015. Evaluation of a commercial electronic nose system coupled with universal gas sensing chamber for sensing indicator compounds associated with meat safety. J. Food Meas. Charact. 9 (2), 121–129.

Paranhos, R.S., Petter, C.O., 2013. Multivariate data analysis applied in Hot-Mix asphalt plants. Resour. Conserv. Recycl. 73, 1–10.

Pearce, T.C., Schiffman, S.S., Nagle, H.T., Gardner, J.W., 2006. Handbook of Machine Olfaction: Electronic Nose Technology. Wiley-VCH, Weinheim.

Persaud, K., Dodd, G., 1982. Analysis of discrimination mechanisms in the mammalian olfactory system using a model nose. Nature 299 (5881), 352–355.

Porier, J.E., Gueit, C., Fanouillet, L., Durand, G., 2009. Laboratory study of environmental performance of binder by headspace gas chromatography. In: Loizos, A., Partl, M.N., Scarpas, T., Al-Qadi, I.L. (Eds.), Advanced Testing and Characterization of Bituminous Materials. CRC Press/Balkema, Taylor & Francis Group, London, pp. 61–68.

RAE System, 2013. The PID Handbook. Theory and Applications of Direct-reading Photoionization Detectors. RAE System, San Jose.

Ropodi, A.I., Panagou, E.Z., Nychas, G.-J.E., 2016. Data mining derived from food analyses using non-invasive/non-destructive analytical techniques; determination of food authenticity, quality & safety in tandem with computer science disciplines. Trends Food Sci. Technol. 50, 11–25.

Rubio, M. del C., Moreno, F., Martinez-Echevvarìa, M.J., Martinez, G., Vàsquez, J.M., 2013. Comparative analysis of emissions from the manufacture and use of hot and half-warm mix asphalt. J. Clean. Prod. 41, 1–6.

Scott, S.M., James, D., Ali, Z., 2006. Data analysis for electronic nose system. Microchim. Acta 156 (3–4), 183–207.

Stimilli, A., Virgili, A., Giuliani, F., Canestrari, F., 2016. In plant production of hot recycled mixtures with high reclaimed asphalt pavement content: a performance evaluation. RILEM Bookseries 11, 927–939.

Stuchi Cruz, S., Paulino, S., Paiva, D., 2017. Verification of outcomes from carbon market under the clean development mechanism (CDM) projects in landfills. J. Clean. Prod. 142, 145–156.

Talaiekhozani, A., Bagheri, M., Goli, A., Reza, M., Khoozani, T., 2016. An overview of principles of odor production, emission, and control methods in wastewater collection and treatment systems. J. Environ. Manag. 170, 186–206.

The Asphalt Institute and Eurobitume, 2015. The Bitumen Industry - a Global Perspective. Production, Chemistry, Use, Specification and Occupational Exposure, third ed. Printed in USA.

Ventura, A., Lorino, T., Le Guen, L., 2015. Modeling of Polycyclic Aromatic Hydrocarbons stack emissions from a hot mix asphalt plant for gate-to-gate Life Cycle Inventory. J. Clean. Prod. 93, 151–158.

Villarrubia, G., De Paz, J.F., Pelki, D., de la Prieta, F., Omatu, S., 2017. Virtual organization with fusion knowledge in odor classification. Neurocomputing 231, 3–10.